VIBRATION SUPPRESSION OF A CANTILEVER BEAM BY OPEN-LOOP CONTROL OF AN ATTACHED STIFFNESS ELEMENT

Bernhard Petermeier and Horst Ecker
Institute of Mechanics and Mechatronics
Vienna University of Technology, Austria
bernhard.petermeier@tuwien.ac.at, horst.ecker@tuwien.ac.at

Abstract

This is a numerical study about new results on the dynamic stability of a beam structure. A uniform cantilever beam with a stiffness element attached to it is investigated. It is assumed that the stiffness parameter of the attached element can be changed periodically with time. Linear and non-linear properties of the stiffness element are considered. The beam structure is discretized by a Finite Element approach. The equations of motion describing the planar vibrations of the beam structure lead to a system with a time-periodic stiffness coefficient. The stability of the linearized system is investigated by a numerical method based on Floquet's theorem. Numerical simulation is employed to calculate time series of the transient beam deflections for the linear and the non-linear case.

It is demonstrated that suppression of free vibrations can be more effective, if the frequency of the periodic stiffness variation is that of a non-resonant parametric combination resonance frequency. Numerical studies show how the location of the attached stiffness element affects the performance of the proposed method. The assumed moderate non-linearity of the stiffness element has almost no effect on the vibrations of the beam, which confirms the useability of simple electromagnetic devices to realize parametric stiffness excitation.

Key words

Parametric resonance, damping, cantilever beam, open-loop control, vibration suppression

1 Introduction

A time-periodic force acting on a beam structure may create various dynamical effects, depending on the direction of the force and the direction of the dominant resulting motion. If such a force is generated by a stiffness element which changes properties periodically, such systems are classified as parametrically excited systems (PE-systems), see [Cartmell, 1990].

Numerous studies have focused in the past on parametrically excited systems and structures because of the interesting phenomena which may occur in such systems. For example, if the frequency of a time-periodic parameter variation is twice the value of a natural frequency of the system, a dynamic instability with unbounded amplitudes (in the linear case) may occur. This phenomenon is commonly termed *parametric resonance* although it is caused by a loss of stability. Interestingly, this effect may also occur for combinations of two or more natural frequencies and is then known as *parametric combination resonance* [Cartmell, 1990]. Because the loss of stability may create severe problems, almost all investigations were focused on those cases, where the combination resonances appeared to be resonant. Since the non-resonant cases were not dangerous they did not seem to be worth of further investigations. For instance, reference [Yeh and Kuo, 2004] is a recent experimental study, which investigates a beam system very similar to the one used in this numerical investigation. Several instability regions (parametric resonances) of a composite beam under parametric excitation are identified and compared with analytical results. The stable (non-resonant) parametric combination resonances, however, are not investigated.

The misinterpretation about the insignificance of stable parametric resonances became obvious when Tondl discovered and reported that a non-resonant parametric combination resonance exhibits interesting properties, which have not been studied so far [Tondl, 1998]. To summarize the findings in a few words, improved vibration suppression may be observed for a system with parametric excitation at such a frequency. First studies of Tondl and others dealt with self-excited low-dof systems and the newly discovered effect was used to stabilize the otherwise unstable system, see [Tondl and Ecker, 1999]. An extensive overview on parametric excitation as a means to achieve vibration suppression is found in [Ecker, 2003] and a thorough analytical analysis in [Dohnal, 2005]. It is an advantage of this method that the amplitude and the frequency of the stiffness

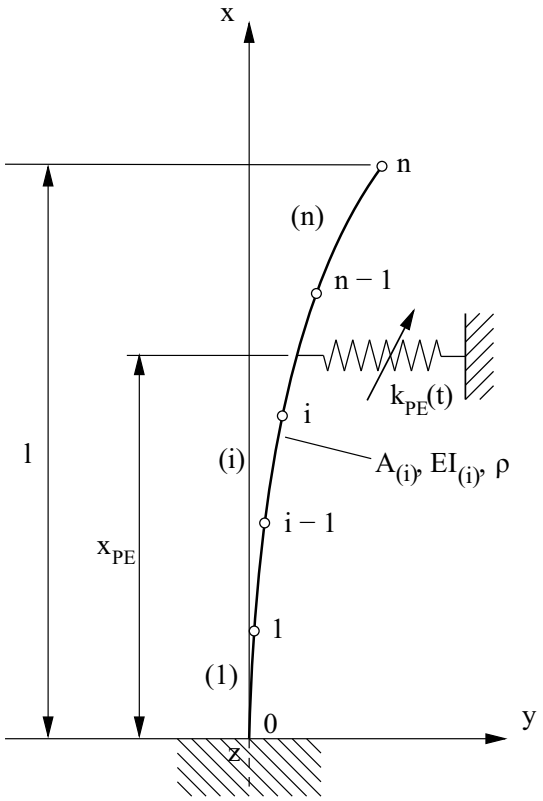

Figure 1. Planar cantilever beam model composed of n finite elements with parametric excitation $k_{PE}(t)$ at $x{=}x_{PE}$

variation can be determined in advance. A signal feedback and a closed loop control is therefore not needed.

The beneficial effect of a parametric stiffness excitation (PSE) at the frequency of a non-resonant parametric combination resonance is not restricted to low-dof lumped mass systems. In [Ecker, Dohnal and Springer, 2005] and [Dohnal, Ecker and Springer, 2005] this idea was already applied to a continuous structure by applying a *time-periodic axial force* to a cantilever beam. It was demonstrated by numerical experiments that free vibrations can be reduced significantly faster by this new approach.

In this contribution we will consider the same one-dimensional continuous system of a cantilever beam, but parametric excitation is achieved by a single, controlled stiffness element attached to the beam.

2 Mathematical model of the mechanical system

Figure 1 shows a cantilever beam which performs planar vibrations in the x-y plane and which is parametrically excited by a single stiffness element $k_{PE}(t)$ attached to the beam at an arbitrary position x_{PE}. The direction of deformation of the stiffness element is perpendicular to the undeflected beam axis. The beam is assembled from n finite bending elements with $n+1$ nodal points $i = 0, 1, 2, ...n$.

Figure 2 shows a finite beam element (i) of length $l_{(i)}$, constant cross section $A_{(i)}$, constant bending stiffness $EI_{(i)}$ and ρ denoting the constant density of the beam material.

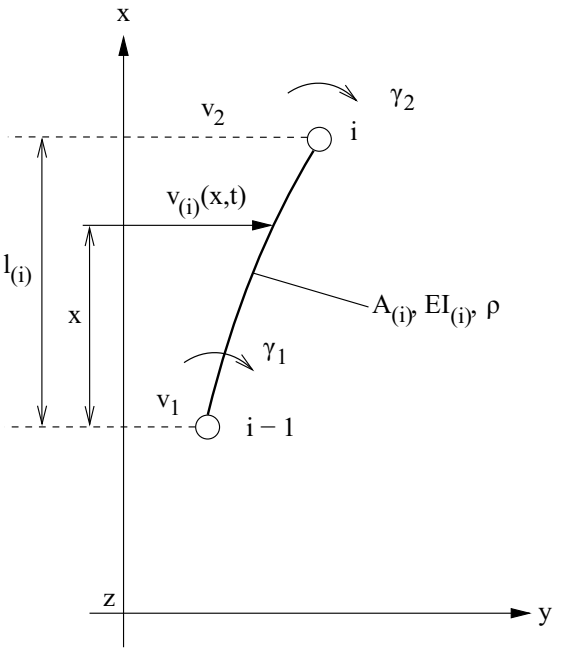

Figure 2. Finite beam element (i) with planar bending deformation

The lateral displacement field $v_i(x,t)$ of a beam element (i) is approximated by Rayleigh-Ritz shape functions in terms of the nodal point displacements v_1, v_2 and the nodal angular deflections γ_1, γ_2 in the form

$$v_{(i)}(\xi,t) = \left[N_1(\xi), N_2(\xi), N_3(\xi), N_4(\xi)\right] \begin{Bmatrix} v_1 \\ \gamma_1 \\ v_2 \\ \gamma_2 \end{Bmatrix}_{(i)} = \mathbf{N}(\xi)\mathbf{q}_{(i)}, \tag{1}$$

where $\xi = x/l_{(i)}$. Functions $N_{1..4}$ represent suitable Hermitian polynomials of third order, see [Géradin and Rixen, 1994], which also satisfy boundary conditions

$$v_{(i)}(0,t) = v_1(t), \tag{2}$$
$$v_{(i)}(1,t) = v_2(t), \tag{3}$$
$$\frac{\partial v_{(i)}(0,t)}{\partial \xi} = l_{(i)}\gamma_1(t), \tag{4}$$
$$\frac{\partial v_{(i)}(1,t)}{\partial \xi} = l_{(i)}\gamma_2(t). \tag{5}$$

2.1 Equations of motion for the cantilever beam

The equations of motion can be derived from d'Alembert´s principle

$$\delta W_I + \delta W_C + \delta W_D + \delta W_{PE} = 0 \tag{6}$$

where δW_I, δW_C, δW_N, and δW_{PE}, respectively, represent the virtual works of inertia forces, conservative (elastic) and non-conservative (damping) forces

and time-periodic (PE) forces in the system. Bernoulli-Euler beam theory is considered, which neglects rotary inertia of the beam cross section.

According to Eq. (1) the virtual work of the inertia forces for each beam element is

$$\delta W_{I(i)} = -\delta \mathbf{q}_{(i)}^T \mathbf{M}_{(i)} \ddot{\mathbf{q}}_{(i)} \tag{7}$$

with the element mass matrix

$$\mathbf{M}_{(i)} = \frac{\rho l_{(i)} A_{(i)}}{420} \begin{bmatrix} 156 & 22l_{(i)} & 54 & -13l_{(i)} \\ & 4l_{(i)}^2 & 13l_{(i)} & -3l_{(i)}^2 \\ & & 156 & -22l_{(i)} \\ symm. & & & 4l_{(i)}^2 . \end{bmatrix} \tag{8}$$

The virtual work of the conservative forces due to a deflection of the beam is related to the potential energy of each beam element. With $\delta W_{C(i)} = -\delta V_{(i)}$ and Eq. (1) it follows

$$\delta W_{C(i)} = -\delta \mathbf{q}_{(i)}^T \mathbf{K}_{B(i)} \mathbf{q}_{(i)} \tag{9}$$

where

$$\mathbf{K}_{B(i)} = \frac{EI_{(i)}}{l_{(i)}^3} \begin{bmatrix} 12 & 6l_{(i)} & -12 & 6l_{(i)} \\ & 4l_{(i)}^2 & -6l_{(i)} & 2l_{(i)}^2 \\ & & 12 & -6l_{(i)} \\ symm. & & & 4l_{(i)}^2 \end{bmatrix} \tag{10}$$

is the finite beam element bending stiffness matrix. Note that the attached time-periodic stiffness element is not considered here and will be treated separately.

From structural dynamics it is known that material damping in the beam may be approximated by internal stiffness-proportional viscous forces. Therefore, the element damping matrix is estimated by

$$\mathbf{C}_{(i)} = \beta \mathbf{K}_{B(i)} \tag{11}$$

with β being an empirical factor.

2.2 Time-periodic stiffness element

Finally, the time-periodic stiffness element $k_{PE}(t)$, which may be attached to any beam element with nodes $(i-1, i)$ at a dimensionless distance ξ from the lower node $(i-1)$, see Figs. 1 and 2, is introduced. Since it is quite simple and convenient to realize parametric stiffness excitation by an electromagnetic device, see [Yeh and Kuo, 2004] and [Schmidt et al., 2007], a non-linear parametric stiffness excitation is assumed. The motivation for a non-linear model is based on the non-linear relationship between magnetic forces and the width of the air gap. In a typical realization of such an electromagnetic PE-device the dynamical properties will be dominated by a constant stiffness parameter plus a component which is a quadratic function of the beam deflection. Thus, the restoring force created by the PE-device will depend primarily in a linear manner on the deflection, and a cubic component will be observed too, leading to a hardening spring behavior.

The potential energy stored in the stiffness element, which is attached to beam element (i), is given by

$$V_{PE(i)} = \frac{1}{2} k_{PE}^{lin}(t) v_{(i)}^2(\xi, t) + \frac{1}{4} k_{PE}^{cub}(t) v_{(i)}^4(\xi, t), \tag{12}$$

with time-periodic coefficients $k_{PE}^{lin}(t)$ for the constant stiffness component and $k_{PE}^{cub}(t)$ for the quadratic component. Note, that the annotation of the coefficients refer to the resulting restoring forces as functions of the deflection only, which is more intuitive in this context.

For both components of the parametric stiffness excitation (PSE) it is assumed that the time-periodic function $k_{PE}(t)$ is a harmonic function, with amplitude $\hat{k}_{PE}$ and frequency η, which may be represented by

$$k_{PE}^{lin}(t) = \hat{k}_{PE}^{lin} \cos(\eta t), \tag{13}$$

$$k_{PE}^{cub}(t) = \hat{k}_{PE}^{cub} \cos(\eta t). \tag{14}$$

With $\delta W_{PE(i)} = -\delta V_{PE(i)}$ and Eq. (1) it follows

$$\delta W_{PE(i)} = -\delta \mathbf{q}_{(i)}^T \mathbf{K}_{PE(i)} \mathbf{q}_{(i)} \tag{15}$$

where

$$\begin{aligned} \mathbf{K}_{PE(i)} &= k_{PE}^{lin}(t) \mathbf{N}^T \mathbf{N} + k_{PE}^{cub}(t) \mathbf{N}^T \mathbf{N} (\mathbf{I}\mathbf{q}_{(i)})^2 \\ &= k_{PE}^{lin}(t) \mathbf{U}_{PE(i)}(\xi) + k_{PE}^{cub}(t) \mathbf{U}_{PE(i)}(\xi) (\mathbf{I}\mathbf{q}_{(i)})^2 \end{aligned} \tag{16}$$

is the finite element matrix for an attached stiffness element. The constant geometry matrix $\mathbf{U}_{PE(i)}(\xi)$ is a function of the point of attachment of the stiffness element and contains polynomials of order six (maximum). Since it is convenient to calculate the matrix elements numerically, the rather lengthy analytical representation is omitted here for brevity.

The virtual works of all beam elements are added, according to the well known assembling procedure for mass, stiffness, and damping matrices of the free-free beam model. From Fig. 1 the boundary conditions for the clamped end at $x = 0$ are $v_1 = 0$, $\gamma_1 = 0$ for the first element $(i) = (1)$, i.e. the first two rows and the first two columns of the assembled matrices have to be omitted. Then Eq. (17) finally leads to

$$\begin{aligned} -\delta \mathbf{q}^T \mathbf{M} \ddot{\mathbf{q}} - \delta \mathbf{q}^T \beta \mathbf{K}_B \dot{\mathbf{q}} - \delta \mathbf{q}^T \mathbf{K}_B \mathbf{q} - \\ - \delta \mathbf{q}^T \mathbf{K}_{PE}(\mathbf{q}, t) \mathbf{q} = 0 \end{aligned} \tag{17}$$

where $\mathbf{M}$, $\mathbf{K}_B$ and $\mathbf{K}_{PE}(\mathbf{q}, t)$ are $(2n \times 2n)$-dimensional symmetric mass and stiffness matrices, respectively for the entire cantilever beam and

$$\mathbf{q} = \{v_1, \gamma_1, v_2, \gamma_2, ...v_n, \gamma_n\}^T \tag{18}$$

is the global beam displacement vector containing lateral displacements v_i and slope angles γ_i at the finite element nodal points.

With Eq. (17) the full set of equations of motion for the non-linear system finally becomes

$$\mathbf{M}\ddot{\mathbf{q}} + \beta\mathbf{K}_B\dot{\mathbf{q}} + \mathbf{K}_B\mathbf{q} + + k_{PE}^{lin}(t)\mathbf{U}_{PE}\mathbf{q} + k_{PE}^{cub}(t)\mathbf{U}_{PE}(\mathbf{Iq})^2\mathbf{q} = \mathbf{0}. \tag{19}$$

3 Parametric resonance frequencies

A system with parametric stiffness excitation (PSE) at a frequency η_{PSE} may exhibit *Principle Parametric Resonances* at frequencies $\eta_{PSE} = \eta_{j/n}^{pr}$ and *Parametric Combination Resonances* at frequencies $\eta_{PSE} = \eta_{j\pm k/n}^{cr}$. These frequencies are defined as follows

$$\eta_{j/n}^{pr} = \frac{2\Omega_j}{n}, \qquad \eta_{j\pm k/n}^{cr} = \frac{|\Omega_j \pm \Omega_k|}{n}, \qquad (j,k = 1,2),\ (n = 1,2,3,...). \tag{20}$$

Symbols Ω_j and Ω_k denote the j-th (k-th) natural frequency of the system. The denominator n represents the order of the parametric resonance. In most cases only the first order resonances $n = 1$ are significant. Instability of a system may occur at and in the vicinity of these frequencies, except for non-resonant PE-frequencies, as discussed in Section 1.

To predict parametric resonances and also the appropriate PSE-frequency for vibration suppression it is necessary to know the natural frequencies of the cantilever beam. Therefore, the undamped natural frequencies Ω_i have to be calculated for the system by solving the eigenvalue problem for $\mathbf{M}\ddot{\mathbf{q}} + \mathbf{K}_B\mathbf{q} = \mathbf{0}$. Note that the time-periodic stiffness element as introduced in Section 2.2 exhibits a zero average value and therefore does not contribute in this analysis to the constant stiffness matrix $\mathbf{K}_B$. For the symmetric stiffness matrix $\mathbf{K}_B = \mathbf{K}_B^T$ parametric vibration suppression will occur for the difference-type combination resonance $\eta_{(2-1)/1}^{cr} = (\Omega_2 - \Omega_1)$ and an interval of instability will be observed at the summation-type combination resonance $\eta_{(1+2)/1}^{cr} = (\Omega_1 + \Omega_2)$. Of course, resonances and non-resonances of higher order $(n \geq 2)$ as well as such resulting from combinations of higher natural frequencies $(\Omega_i, i > 2)$ may exist, but are not investigated in this study.

4 Method of investigation

A non-linear system of differential equations with periodic coefficients is defined by Eq. (19) in combination with matrices (8), (10), (16) and functions (13) and (14). The stability of the trivial solution $\mathbf{q} = \mathbf{0}$ for the linearized system can be investigated by means of Floquet-theory, see [Verhulst, 2000]. Floquet's theorem postulates that for a system of first order differential equations

$$\dot{\mathbf{y}} = \mathbf{A}(t)\,\mathbf{y}, \qquad \mathbf{A}(t) = \mathbf{A}(t+T), \tag{21}$$

with a T-periodic matrix $\mathbf{A}(t)$ each fundamental matrix $\mathbf{M}(t)$ of the system can be represented as a product of two factors

$$\mathbf{M}(t) = \mathbf{Q}(t)\exp(t\mathbf{C}), \tag{22}$$

where $\mathbf{Q}(t)$ is a T-periodic matrix function and $\mathbf{C}$ is a constant matrix.

Stability of a linear time-periodic system can be determined either from the eigenvalues of the *Floquet exponent matrix* $\mathbf{C}$ or from the *monodromy matrix* $\mathbf{M}(T)$, which is the state transition matrix evaluated after a period T. The monodromy matrix can be calculated numerically by repeated integration of the system equations over one period T, starting from independent sets of initial conditions. It is convenient to use the columns of the identity matrix $\mathbf{I}$ as initial vectors to start from. By solving n initial value problems over one period T

$$\dot{\mathbf{y}} = \mathbf{A}(t)\mathbf{y}, [\mathbf{y}(0)_1, \mathbf{y}(0)_2, ..., \mathbf{y}(0)_n] = \mathbf{I}, t = [0,T], \tag{23}$$

and by arranging the results as follows

$$\mathbf{M}(T) = [\mathbf{y}(T)_1, \mathbf{y}(T)_2, ..., \mathbf{y}(T)_n] \tag{24}$$

the monodromy matrix is obtained. Finally the eigenvalues of the monodromy matrix

$$\mathbf{\Lambda} = \text{eig}(\mathbf{M}(T)), \tag{25}$$

are calculated numerically. The system is unstable if any of the eigenvalues are larger than one in magnitude

$$\max(|\Lambda_1|, |\Lambda_2|, ..., |\Lambda_n|) \quad \begin{cases} < 1 \text{ stable system} \\ > 1 \text{ unstable system.} \end{cases} \tag{26}$$

To carry out the stability analysis and obtain the following results, Eq. (19) was linearized first by omitting the non-linear contribution $(k_{PE}^{cub}(t) = 0)$. Then a first order system (21) was generated and the procedure as outlined was applied.

5 Results from a stability analysis

For the following numerical study the same data for a slender and uniform cantilever beam were used as in [Ecker, Dohnal and Springer, 2005] and [Dohnal, Ecker and Springer, 2005]. This enables the comparison of results obtained from two different methods to create parametric stiffness excitation. Table 1 lists the size and mechanical properties of the beam structure as investigated.

Parameter	Symbol	Value	Units
Length	l	1	m
Cross section	A	5×10	mm^2
Density	ρ	7850	kg/m^3
Young's Modulus	E	210	GPa
Damping factor	β	$0.77 \cdot 10^{-3}$	sec
Gravitational forces are not considered in this example			

Table 1. Mechanical parameters of the cantilever beam

Frequency	Value	Units	FEMs
Ω_1	26.23 (26.22)	sec^{-1}	6
Ω_2	164.41 (164.36)	sec^{-1}	6
Ω_3	461.07 (460.26)	sec^{-1}	6
$2\Omega_1$	52.46	sec^{-1}	6
$\Omega_2 - \Omega_1$	138.18	sec^{-1}	6
$\Omega_1 + \Omega_2$	190.63	sec^{-1}	6

Table 2. Natural frequencies of the undamped cantilever beam, obtained for a model with 6 FEMs. Values in parentheses hold for the analytic solution.

In this numerical study the beam structure is discretized by 6 identical finite beam elements (FEMs), see Section 2. The number of elements was chosen to obtain a good agreement for the lowest three natural frequencies with regard to the FE-model and the analytical result. Table 2 shows the natural frequencies obtained for a 6-element model and also for an analytical solution as the reference. There is no need to further increase the number of elements for studies as carried out here. This can be concluded from the results obtained in [Dohnal, Ecker and Springer, 2005] which employs only four finite beam elements and achieves almost identical results as the study in [Ecker, Dohnal and Springer, 2005]. Hence, it can be concluded that the following results are representative and practically not affected by the level of discretization.

Parametric excitation (PE) is achieved by a stiffness element with time-periodic parameter values as defined by Eqs. (13),(14). Note that $k_{PE}(t)$ has no constant component and therefore will take on also negative values. PE-amplitudes $\hat{k}_{PE}^{lin}$, $\hat{k}_{PE}^{cub}$ and frequency η, as well as the position x_{PE} will be subject of parameter studies in the following investigations.

At first, the stability of the parametrically excited linear system is investigated by the numerical method explained. Figure 3 shows how the largest eigenvalue of the monodromy matrix depends on the PE-frequency. One can easily identify rather large intervals of instability near $2\Omega_1 = 52.5$ and also near

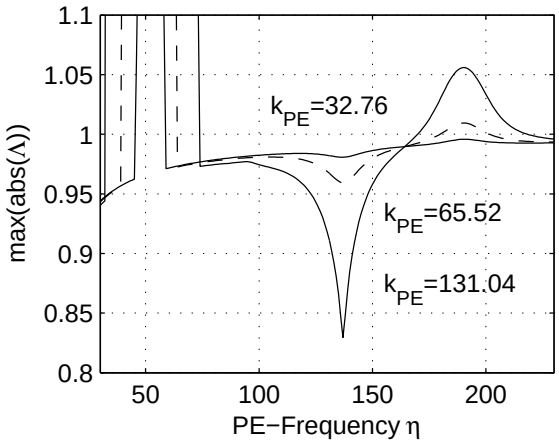

Figure 3. Largest absolute eigenvalue of the monodromy matrix $\max(|\Lambda_i|)$ as a function of the PE-frequency η for various values (N/m) of $\hat{k}_{PE}^{lin}$.

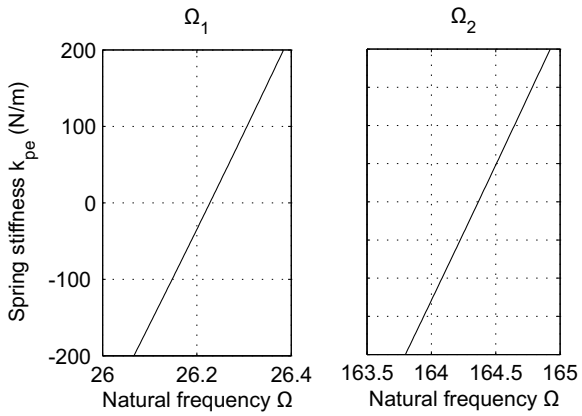

Figure 4. First natural frequencies of the cantilever beam if a time-independent (constant) stiffness is attached to the tip of the beam (l=1).

$\Omega_1 + \Omega_2 = 190.6$, where the maximum eigenvalue exceeds 1 $(\max(\text{abs}(\Lambda)) > 1)$. In the vicinity of $\Omega_2 - \Omega_1 = \eta \simeq 138$ a decrease of the largest eigenvalue is observed, indicating enhanced stability of the system. For this diagram it is assumed that the linear PE-stiffness element is attached to the top of the beam ($x_{PE} = l$). Three different values are chosen for $\hat{k}_{PE}^{lin} = [0.5 * 65.52, 65.52, 2 * 65.52]$, while $\hat{k}_{PE}^{cub} = 0$. The choice for the coefficient of the linear parameter is based on the bending stiffness $k_B(l) = 65.52$ N/m at the top node $x_{PE} = l = 1$ m of the beam and relates the bending stiffness to the PSE-amplitude.

Since the natural frequencies of the system also become periodic functions of time when parametric stiffness excitation is introduced, it is interesting to check how these natural frequencies change, when the maximum time-periodic value is reached. In Fig. 4 the sensitivity of the first and most important natural frequencies are shown. As we will use later amplitudes for the linear parametric stiffness excitation within the range shown in Fig. 4, one can see that the variation of the natural frequencies will be quite insignificant and not really important in this study.

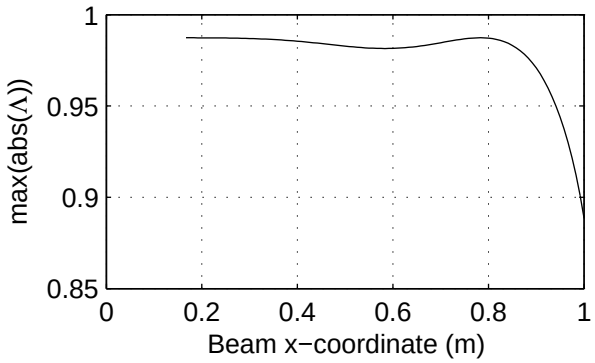

Figure 5. Largest absolute eigenvalue of the monodromy matrix $\max(|\Lambda_i|)$ as a function of the PE-location x_{PE} for $\hat{k}_{PE}^{lin}$= 113.22 N/m

The optimal point for attaching a PE-stiffness element with $\hat{k}_{PE} \leq 3 * k_B(l)$ is the tip of the beam. Figure 5 shows for $\hat{k}_{PE} = 113.22$ N/m how the largest eigenvalue depends on the location where the PE-stiffness element is attached to the beam, with an absolute minimum at $x_{PE} = l = 1$ m.

For a cantilever beam the familiar formula

$$k_B(x) = \frac{3EI}{x^3} \tag{27}$$

holds and shows that the bending stiffness increases with the third power, for decreasing length of the beam. One cannot expected that a rather small but still effective stiffness amplitude at $x_{PE} = l$ will give also satisfactory or even better results at $x_{PE} < l$. Therefore, the amplitude $\hat{k}_{PE}$ is set into relation to the bending stiffness at the point of attachment $k_B(x_{PE})$.

Figure 6 shows a diagram for the the largest eigenvalue as a function of the position x_{PE} and also the frequency η. In this diagram $\hat{k}_{PE}^{lin} = k_B(x_{PE})$, $\hat{k}_{PE}^{cub} = 0$ holds, which means that larger PE-amplitudes are used as the position of attachment moves away from the tip of the beam. One can see from this diagram that near $x_{PE} \simeq 5l/6$ almost no reduction of the eigenvalue can be achieved and hence increased damping cannot be

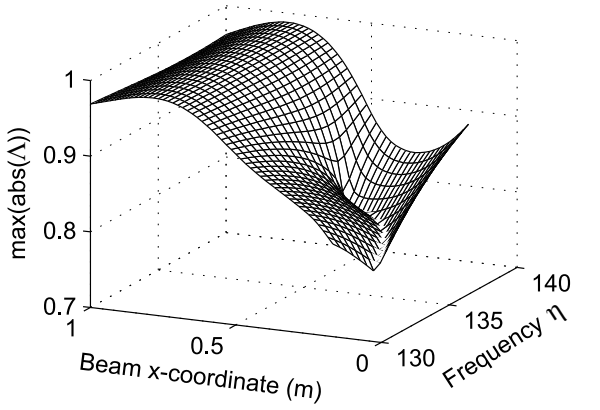

Figure 6. Largest absolute eigenvalue of the monodromy matrix $\max(|\Lambda_i|)$ as a function of the PE-frequency η and the PE-location x_{PE} for $\hat{k}_{PE}^{lin}$=$k_B(x_{PE})$

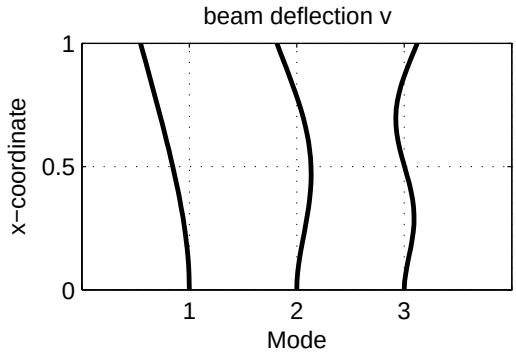

Figure 7. Mode shapes of the cantilever beam investigated in this study

expected. For $l/3 > x_{PE} > l/6$, however, a major reduction of the eigenvalue is observed which exceeds the result for $x_{PE} = l$ by far.

It was shown, that a significant reduction of the largest eigenvalue of the monodromy matrix, which determines the stability of the cantilever beam, can be achieved by parametric excitation at a difference-type combination frequency. This result, however, cannot be converted easily into a familiar damping measure. Therefore, we will now investigate the beam structure in the time domain, to show how this affects and enhances the damping properties of the structure.

6 Results obtained in the time domain

Since the beam structure can be represented by a linear model, it is convenient to analyze first the lowest vibrational modes of the linear-time-invariant (LTI)-system, and then use these results as a benchmark for the parametrically excited structure.

In Fig. 7 the corresponding mode shapes are plotted. The first three natural frequencies of the undamped structure have been listed already in Table 2. The damping ratios for these modes are $\zeta_1 = 0.01$, $\zeta_1 = 0.063$ and $\zeta_1 = 0.178$ for the damping factor β, as introduced in Eq. (11). Note that stiffness-proportional damping leads to significantly higher damping ratios for higher modes.

Figures 8 show time series of the lateral deflections $v_{3,6}$ at the nodal points 3 and 6 of the beam. Point 3 is located at the mid-span position $x = l/2$ and point 6 is at the tip of the beam. The first mode shape was assumed as an initial deflection of the beam, the initial velocity was set to zero. These initial conditions only excite the first vibrational mode and consequently a single-frequency harmonic vibration at (almost) Ω_1 is observed. Deflections at point 3 and point 6 are in phase, according to the first mode shape. Without parametric stiffness excitation the vibration in Fig. 8(top) decays pretty slowly, since the damping ratio is just 1%, ($\zeta = 0.01$). For Fig. 8(bottom) parametric excitation is applied to the beam structure and the numerical study is repeated in the same manner as before. For the parameters of the parametric excitation the parameter

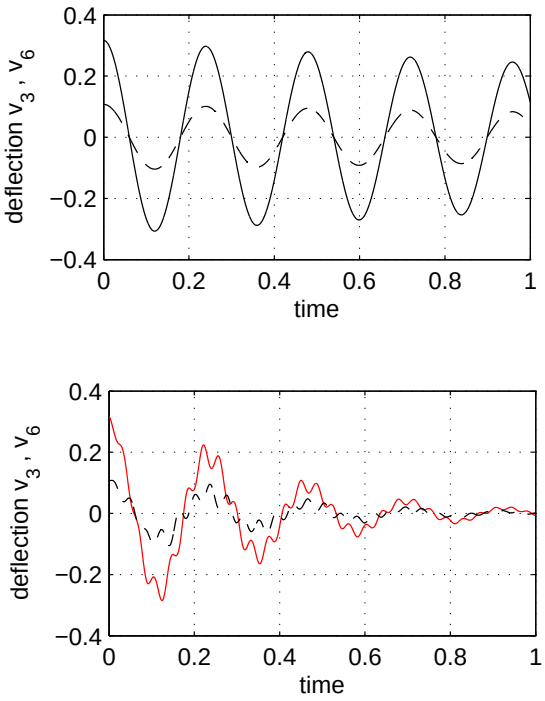

Figure 8. Transients of weakly damped beam (β=0.77·10^{-3}) for 1^{st} mode initial condition. Top: without PE. Bottom: with linear PE (η=138,$\hat{k}_{PE}^{lin}(l)$=131.04 N/m). Solid line - node 6, dashed line - - node 3.

values $\eta = 138.0$, $\hat{k}_{PE}^{lin}(l) = 131.04$N/m, were chosen. The amplitude of the parametric stiffness excitation is set to a value of twice the bending stiffness of the cantilever beam if deflected at the tip of the beam. This seems to be a reasonable and realistic assumption for the performance of the electromagnetic device to create the parametric stiffness excitation. It is clearly to see that the initial vibrations decay much faster, compared to the result without PE. It is also remarkable, that a vibration component of higher frequency is observed, which is not contained in the initial state of the numerical experiment. Further analysis shows that second mode vibrations are generated by the parametric stiffness excitation and contribute to the rapid decay of vibrations. Concluding from related results in the earlier study [Ecker, Dohnal and Springer, 2005] on the axially excited beam, the effect of the parametric stiffness excitation is approximately equivalent to an increase of the damping of the first vibrational mode by a factor of ten.

In Fig. 9 results are shown for non-linear parametric stiffness excitation. Figure 9 (top) assumes a non-linear component in addition to the linear PE with a parameter value for the cubic coefficient of $\hat{k}_{PE}^{cub}(l) = 131.04$ N/m^3. With a coefficient of this value a very weak non-linearity is introduced, since the restoring force of the cubic component will reach the same amount as the linear component only when the deflection would become 1 meter. Moreover, a cubic parabola has a horizontal tangent and vanishing curvature for $x = 0$. Therefore, after linearization of the restoring force function the cubic component will disappear without any contribution. Consequently, it has to be expected that the non-linear parametric stiffness excitation will have only very little effect on the result. Indeed, if one compares Fig. 9 (top) with Fig. 8(bottom) there is no difference visible. Closer inspection of the numerical data show, of course, some differences, which are not visible in the plots. Therefore, the non-linear parameter was increased by a factor of ten and the result Fig. 9 (bottom) was obtained. Even for this parameter set only minor differences are observed. Of course, with the numerical model it is easy to further increase the non-linear component and demonstrate the effect of nonlinearity for larger values of the parameters. However, we will postpone such an investigation until actual parameters for a PSE-device are available and a realistic design study suggests to further increase the non-linear parameter value.

The final result and figure is devoted to second mode vibrations. In Fig. 10 it is assumed that the initial deflection of the beam is the 2^{nd} mode. Figure 10 (top) holds for linear PE and Fig. 10 (bottom) for the same parameters of a weak nonlinearity as in Fig. 9 (top). Again in this comparison the cubic nonlinearity has practically no influence on the results. The qualitative behavior of the system, however, is different for initial conditions favoring the 2^{nd} mode. Immediately after the vibrations start, within one second a few vibration

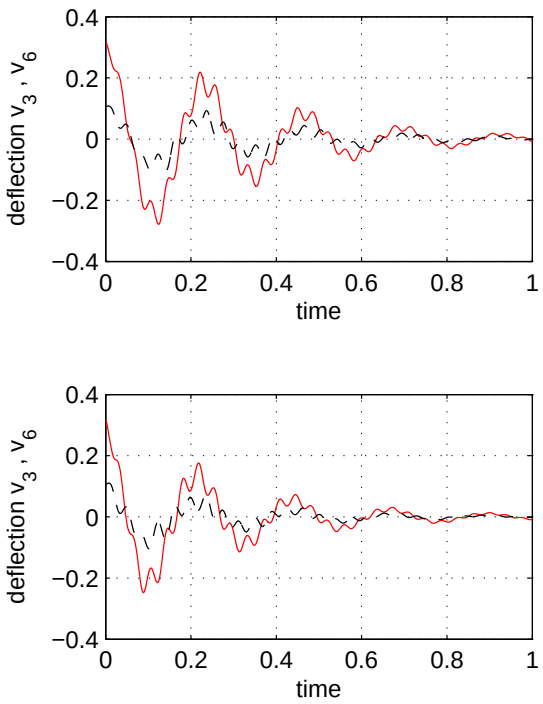

Figure 9. Transients of weakly damped beam (β=0.77·10^{-3}) for 1^{st} mode initial condition, with non-linear PE (η=138,$\hat{k}_{PE}^{lin}(l)$= 131.04 N/m). Top: $\hat{k}_{PE}^{cub}(l)$=131.04 N/m^3 Bottom: $\hat{k}_{PE}^{cub}(l)$= 1310.4 N/m^3. Solid line - node 6, dashed line - - node 3.

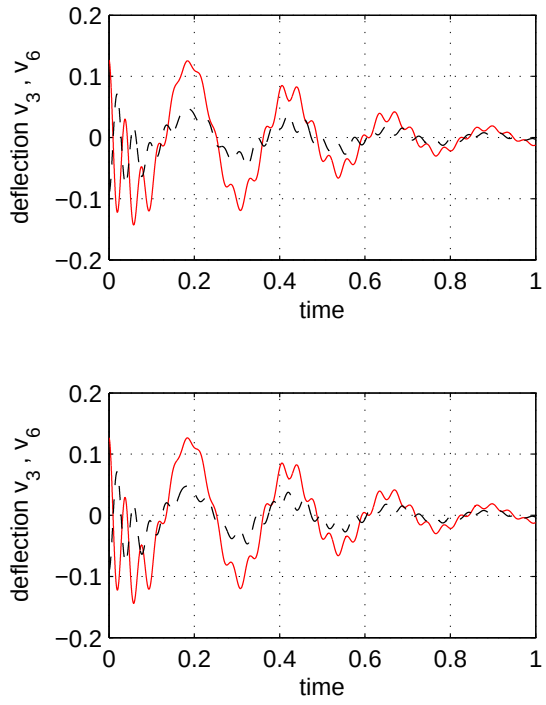

Figure 10. Transients of weakly damped beam (β=$0.77{\cdot}10^{-3}$) for 2^{st} mode initial condition. Top: with linear PE (η=138,$\hat{k}_{PE}^{lin}(l)$= 131.04 N/m). Bottom: with non-linear PE (η=138,$\hat{k}_{PE}^{lin}(l)$= 131.04 N/m, $\hat{k}_{PE}^{cub}(l)$=131.04 N/m^3). Solid line - node 6, dashed line - - node 3.

cycles are performed with the frequency of the second mode. Then second mode vibrations decay fast, but first node vibrations appear and become dominant. Obviously, an energy transfer from the second to the first mode takes place, which is initiated by parametric stiffness excitation. After about 0.5 seconds the vibration signals become quite similar to those obtained for the first mode initial conditions.

7 Conclusion

In this numerical study new findings on parametric resonances are presented. It is demonstrated, that a parametrically excited beam structure exhibits enhanced damping properties, when excited by a non-resonant parametric combination resonance frequency. The damping effect achievable by this method is significant and works best for vibrations in the first mode of the structure. A mild od moderate non-linear behavior of the device to create the time-periodic stiffness has no negative effect on the damping effect created by a non-resonant parametric excitation.

The striking advantage of the method presented is the fact that parametric excitation only needs an open-loop control system. This might be very advantageous for real-world applications, since it will save the cost, weight and energy for sensors and controllers, which might be very important in certain applications.

References

Cartmell, M. (1990). *Introduction to Linear, Parametric and Nonlinear Vibrations.* Chapman and Hall, London.

Chen, C.-C. and Yeh, M.-K. (1995) Parametric instability of a cantilevered column under periodic loads in the direction of the tangency coefficient. *JSV*, **183**(2), pp. 253–267.

Dohnal F. (2005). *Damping of Mechanical Vibrations by Parametric Excitation.* Ph.D. Thesis, Vienna University of Technology.

Dohnal F., Ecker H. and Springer, H. (2007). Enhanced Damping of a Cantilever Beam by Axial Parametric Excitation. *Arch. Appl. Mech.*, Springer online, pp. 1–13.

Ecker H. (2003). *Suppression of Self-excited Vibrations in Mechanical Systems by Parametric Stiffness Excitation.* Habilitation Thesis, Vienna University of Technology.

Ecker H., Dohnal F. and Springer, H. (2005). Enhanced Damping of a Beam Structure by Parametric Excitation. In *Proc. of Fifth EUROMECH Nonlinear Dynamics Conferences (ENOC-2005)*, Eindhofen, Netherlands, Aug. 7-12, Paper 22-271, 10p.

Geradin, M. and Rixen, D. (1994). *Mechanical Vibrations - Theory and Application to Structural Dynamics*. Wiley, New York, and Masson, Paris.

Habib, M.S. and Radcliffe, C.J. (1991) Active Parametric Damping of Distributed Parameter Beam Transverse Vibration. *J. Dynamic Systems, Measurement, and Control*, **113**, pp. 295–299.

Iwatsubo, T., Sugiyama, Y. and Ogino, S. (1974) Simple and combination resonances of columns under periodic axial loads. *JSV*, **33**, pp. 211–221.

Schmidt, E., Paradeiser, W., Dohnal, F., Ecker, H.: *Design of an electromagnetic actuator for parametric stiffness excitation.* COMPEL **26**, 3, pp. 800–813, 2007.

Tondl A. (1998). *To the problem of quenching self-excited vibrations.* Acta Technica CSAV **43**.

Tondl A., Ecker H. (1999). *Cancelling Of Self-Excited Vibrations By Means Of Parametric Excitation.* Proc. 1999 ASME Design Engineering Technical Conferences (DETC), Sept. 12-15, 1999, Las Vegas, Nevada, USA.

Verhulst, F. (2000). *Nonlinear Differential Equations and Dynamical Systems*. Springer-Verlag.

Yeh, M.-K. and Yao-Ting Kuo (2004) Dynamic instability of composite beams under parametric excitation. *Composite Science and Technology*, **64**, pp. 1885–1893.